
COMPUTER BASED IDENTIFICATION OF DIABETES RETINOPATHY USING TEXTURE PARAMETERS

Sagar S. Lachure
Asst. Prof at Ycce Nagpur

Jaykumar S. Lachure
Student at GCOE Amravati

Swati D. Gupta
Student at RKNEC Nagpur

Abstract

Diabetic retinopathy is one of the diabetes-implicated diseases that are one of the major causes of preventable blindness in the world. It occurs when there is high concentration of glucose in the small blood vessels in the retina, damaging the eye and result in blurred vision or even blindness. For proper medical treatment and control to prevent condition from deteriorating, regular screening is essential in diagnosing the stages of diabetic retinopathy at an early stage

Various methods have been researched with the common objective to achieve a cost and time effective classification of the fundus images to provide an immediate diagnosis of the retina, compared with the conventional method of using a specialised medical personnel in the visual identification of the images which is time consuming. With the increase number of people being diagnosed with the condition, the demand for eye screening will inevitably increase and so is the amount of images needed to be screen for diagnosis. Most automated identification methods are structural based analysis where classification is based on identification and recognition of patterned texture features.

Keywords: texture, fundus, diagnosis, retina.

Introduction

Diabetes mellitus is a chronic diseases characterized by high level of glucose content in the blood. This is a result of insufficient production on insulin by the pancreas or the resistant of insulin by the body. Subsequently, this will cause hyperglycaemia and thus potentially damaging the human body's system, especially to the nerve and blood vessel. Over time, the complication of diabetes mellitus will eventually damage the body organs such as the kidney, heart, nervous system or the eye. These are usually the result of the damage caused by the diseases to small or large blood vessels. Today, diabetes affects 285 million people globally, which make up of 6.6% of the world population. A study by the International Diabetes Federation projects an approximate 438.4 million people to be diagnosed with the chronic diseases by the year 2030, a 54% projected increase against the current numbers [1]. In Singapore, diabetes mellitus affects 8.2% of the population from the ages ranging as young as 18 to 69 years old [2].

Currently, with the advancement of medical imaging and technology, images of the retina could be taken with a fundus camera, a specialised low power microscope to photograph the interior surface of the eye. Identification of the various stages of diabetic retinopathy such as normal, non-proliferative diabetic retinopathy (NPDR), proliferative diabetic retinopathy (PDR) will require a specialist to identify and diagnose. In the aim to provide cost and time effective diagnosis, automated identification of fundus image was developed using feature pattern recognition in the classification. Many image pre-processing methods and mathematical algorithms are required in such system. Hence a statistical approach of the classification will be beneficial to the study of automated identification of the fundus images as it could provide a more time and cost effective alternative in processing large amount of data.

This paper is structured explained part 2 This section start with a brief discussion on the eye's structure and DR in relation to the eye and shortly followed by review of some of the past work done on detecting and classifying DR into crossover points, red spots and bleedings. part 3 and 4 of scetion starts with introduction to basic image processing techniques used in this work, these include Colour Space Conversion, Histogram Equalization, Median Filtering and Morphological Operation on retinal fundus images.Part 5 In this part the stages involve in DR diagnosis are discussed. These stages include Pre-processing, Segmentation, Disease Classifiers/Abnormalities Detection. Also include result comparison with other method part 6 Results of this work are shown.Part 7 gives Conclusion and future work.

Literature survey

The anatomy of the human eye is shown in Figure 1. When light enters the pupil, the lens will focus it and then detected by the retina. The amount of light entering the eye will be regulated by the iris. The movement of the iris is controlled by the contraction and relaxation of the ciliary muscle. The retina contains light-sensitive receptors consisting of rods and cones. As rods are more sensitive and require less light to function, they are used mostly in the night or dim places with poor visibility. Unlike the characteristic of rods, cones are less sensitive and are normally used in daylight for perception of colour. Upon detected by the retina, electrical signal will be delivered to the brain by the optic nerve. Finally, these impulses will be translated into images that we perceived. The macula is located in the centre of the retina and this is responsible for providing a central vision [6]. Also, the fovea is located within the macula and this location provides the sharpest vision and colour perception.

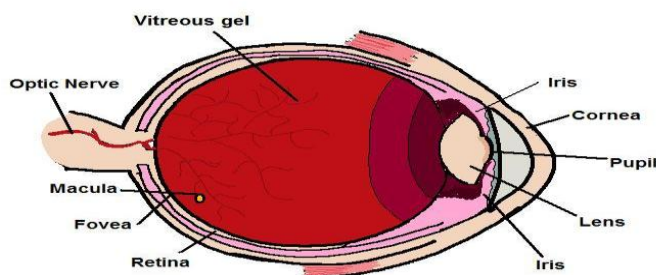


Figure 1: Anatomy of the eye

There are a total of 4 stages in diabetic retinopathy.

- Mild Non-Proliferative Diabetic Retinopathy (Mild NPDR): Presence of small-balloon-like swelling known as microaneurysms and haemorrhages.
 - Moderate Non-Proliferative Diabetic Retinopathy (Moderate NPDR): Blood vessels which are responsible for transportation of nutrients and oxygen are blocked off. This results in more microaneurysms and haemorrhages.
 - Severe Non-Proliferative Diabetic Retinopathy (Severe NPDR): As more blood vessels are blocked, a signal will be sent to the brain requesting for more oxygen. This results in the growth of more but fragile blood vessels.
 - Proliferative Diabetic Retinopathy (PDR): This is the advance stage of the disease. The new blood vessels grow along the retina and gel inside the eyes. Due to the weak structure of the vessels, the blood may leak in the eye and cause severe vision loss. The end-result is blindness.

Using the current technology, large amounts of fundus images are collected from the eye-examination with the fundus camera. These images are sent to trained ophthalmologists for analysis and diagnosis. In order to improve the efficiency of the work process and cost-reduction, there is a demand in the use of computer-based approach to detect diabetic retinopathy stages [7]. Using the current technology, large amounts of fundus images are collected from the eye-examination with the fundus camera. These images are sent to trained ophthalmologists for analysis and diagnosis. In order to improve the efficiency of the work process and cost-reduction, there is a demand in the use of computer-based approach to detect diabetic retinopathy stages [7].

Till present, many methods are researched and developed to increase the sensitivity and specificity. Sensitivity refers to the percentage of abnormal fundus images classified as abnormal by the method used [9]. Specificity is defined as the percentage of normal fundus images classified as normal [9]. When these two factors increase, these indicate that the method is better and more accurate. As a result, a computer-aided diagnosis system to detect different stages of diabetic retinopathy was developed to assist the ophthalmologists. In the study of 25 fundus images conducted by IQbal, M.I, aibinu, A.M, Gubbal, N.S, Khan, A, this system was developed to categorize grade 1 and 2 diabetic retinopathy [9]. With the implementation of equalisation of uneven illumination in the pre-processing stage, the quality of the fundus image improved. Then, k-mean clustering algorithm with two-cluster class centre was carried out in the segmentation stage. Lastly, noisy pixels were removed from the image in the disease classifier stage. From this research, it is able to detect red spots and bleeding successfully with specificity and sensitivity of 98% and 61% respectively. In another research, a three-step approach to detect and classify bright lesion in colour fundus image was carried out by XiaoHui, Z., and Chutatape, O[10]. The approach consists of the following 3 steps: 1) The use of local contrast enhancement, 2) Improved fuzzy C-means to segment bright lesion and 3) Hierarchical support vector machine for classification purposes.

In another research by Vallabha et al [11], the scale and orientation of Selective Gabor filter was used for detection and classification of vascular abnormalities. This is chosen to detect and classify the fundus images into mild or severe case with reference to the output obtained from the Gabor filter.

As shown in Figure 2, this is the proposed system for this study. By using texture image processing technique, five features such as homogeneity, correlation, short run emphasis, long run emphasis and run percentage were extracted and then input to the classifier for automatic identification of normal and diabetic retinopathy cases.

In this work, we will be using 110 fundus images. The 3 different classes are Normal, NPDR and PDR are shown in Figure 2. Mild, moderate and severe NPDR will be classified as one class under NPDR.

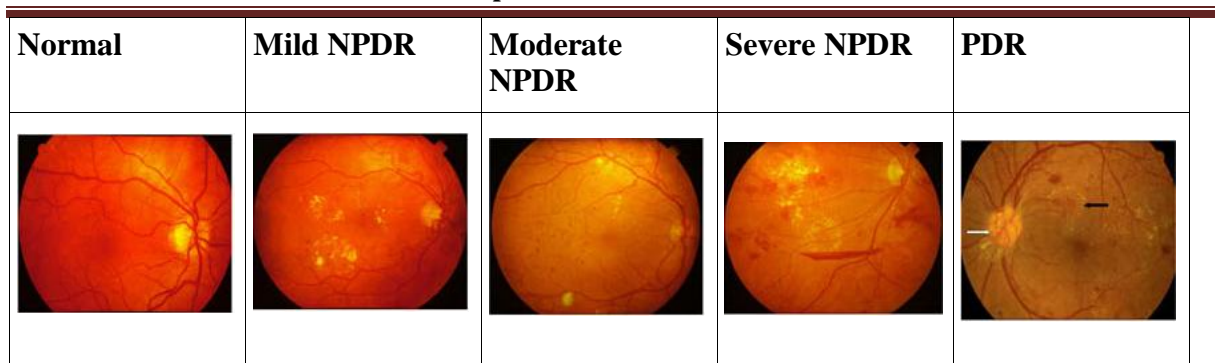


Figure 2: Typical fundus image of 5 different classes [12]

3. Digital Image Processing

Digital images are electronic snapshots of the physical world, either a specific scene or documents such as a photo, a printed text or a piece of artwork design. This physical image is then sampled and mapped into a digitalized image, consisting of a two dimensional array of small square regions called pixels. Image pre-processing is a process to reduce the presence of unwanted features of the image such as noise. The purpose of image pre-processing is to improve the quality of the image being process. As a result, it provides a much accurate results for any image analysis made. Image processing techniques consist of a range of standard image filtering methods such as Median filtering or histogram equalization etc. An image can be represented by a histogram graph that analyse the number of pixels (vertically) with a certain pixel value (horizontally). In essence, an equalized image is represented by an equalized histogram where the number of pixels is spread evenly over the available frequencies. For images which contain varying regions of low contrast bright or dark regions, adaptive histogram equalization method can be use to improve the contrast in the image. It differs from the basic histogram equalization as it considers small regions. Based on their local cumulative distribution frequencies, it performs contrast enhancement in those regions.

Human visual description of a colour object is commonly distinguished by type, degree and brightness. HSI color space decouples the intensity component from the color carrying information in a colour image, providing the intensity component of the image that is most suitable in the processing of image. H stands for hue will define the color, S stands for saturation will define how strong that particular color will be and I the intensities which specified the brightness. [19]

The RGB values of the image are normalize

$$r = \frac{R}{R+G+B}, g = \frac{G}{R+G+B}, b = \frac{B}{R+G+B}$$

Each normalized H,S and I components are then obtain by

$$h = \cos^{-1} \frac{0.5[(r-g) + (r-b)]}{\sqrt{[(r-g)^2 + (r-b)(g-b)]}} \quad h \in [0, \rho] \text{ for } b \leq g$$

$$h = 2\rho - \cos^{-1} \frac{0.5[(r-g) + (r-b)]}{\sqrt{[(r-g)^2 + (r-b)(g-b)]}} \quad h \in [\rho, 2\rho] \text{ for } b > g$$

$$s = 1 - 3(\min(r, g, b)) \quad s \in [0, 1]$$

$$i = (R+G+B)/(3 \cdot 255) \quad i \in [0, 1]$$

4.Texture Features

Texture is a representation of the surface and structure of an image. It is also defined as a common pattern on a surface. Image textures provide information about the spatial arrangement of colours or intensities such as tone variation, shape, size, colour, brightness etc. Texture analysis is a characterization of patterns in an image by their texture content such as rough smooth or shapes. Texture analysis attempts to quantify these texture features as a function of spatial variation in pixel intensities, like representing a rough surface by a variation of the intensity values of the individual pixels in a digital image. Texture analysis is used for segmenting an image into regions with the same texture and recognizing these similar features to classify the objects based on their features. Four major application domains related to texture analysis are texture classification, texture segmentation, shape from texture and texture synthesis.

4.1 Gray Level Co-occurrence Matrix

For an image of size M x N, the gray level co-occurrence matrix (GLCM) is defined as

$$C_d(i, j) = \left| \left\{ (x, y) \mid I(x, y) = i, I(x + \Delta x, y + \Delta y) = j \right\} \right| \quad (1)$$

Where $(\Delta x, \Delta y)$, $d = (\Delta x, \Delta y)$ and $|\cdot|$ denotes the cardinality of a set. Given a grey level i in an image, the probability that the gray level of a pixel at a $(\Delta x, \Delta y)$ distance away is j is

$$P_d(i, j) = \frac{C_d(i, j)}{\sum C_d(i, j)} \quad (2)$$

4.2 Haralick Texture Features

Contrast

$$\sum_i \sum_j (i - j)^2 P_d(i, j)$$

(3)

Contrast is the measurement of the local variations or differences in the GLCM. It works by measuring how elements do not lie on the main diagonal and returns a measure of the intensity contrast between a pixel and the neighbouring pixels over the whole image. Large contrast reflects large intensity difference in GLCM.

Homogeneity

$$\sum_i \sum_j \frac{1}{1 + (i - j)^2} P_d(i, j) \quad (4)$$

Homogeneity measures how close the distribution of elements in the GLCM is to the diagonal of GLCM. Homogeneity weighs values by the inverse of the contrast weight, with weights decreasing exponentially away from the diagonal as shown in equation (4). The addition of value '1' in the denominator is to prevent the value '0' during division. As homogeneity increases, the contrast typically decreases.

Entropy

$$-\sum_{i,j} P_d(i,j) \log P_d(i,j)$$

(5)

Entropy is understood from the concept of thermodynamics. It is the randomness or the degree of disorder present in the image. The value of entropy is the largest when all elements of the co-occurrence matrix are the same and small when elements are unequal.

Energy and Angular Second moment

$$\text{Energy} = \sqrt{\sum_i \sum_j P_d(i,j)^2}$$

(6)

and

$$\text{Angular Second Moment: } \sum_i \sum_j P_d^2(i,j)$$

(7)

Energy is sometimes derived from the use of angular second moment. It is the sum of squared elements in the GLCM known as angular second moment. Basically, it is the measurement of the denseness or order in the image. Moments 1 to 4 are defined as:

$$m_g = \sum_i \sum_j (i - j)^g P_d(i,j)$$

(8)

where g is the integer power exponent that defines the moment order. Moments are the statistical expectation of certain power functions of a random variable and are characterized as follows: moment 1 is the mean which is the average of pixel values in an image; moment 2 is the standard deviation; moment 3 measures the degree of asymmetry in the distribution; and moment 4 measures the relative peak or flatness of a distribution and is also known as kurtosis.

Difference Statistics are defined as the distribution of probability $P_\delta(k)$ ($k = 0, \dots, n-1$), and k is gray level difference between the points separated by δ in an image. They are a subset of co-occurrence matrix and the distribution of probability $P_\delta(k)$ is defined as:

$$P_\delta(k) = \sum_i \sum_j c_d(i,j)$$

(9)

Four such features are computed as follows.

Angular second moment

$$\text{(ASM): } \sum_{k=0}^{n-1} P_\delta(k)^2$$

(10)

When the $P_\delta(k)$ values are very similar or close, ASM is small. ASM is large when certain values are high and others are low.

Contrast

$$\sum_{k=0}^{n-1} k^2 P_\delta(k)$$

(11)

Contrast is also known as the second moment of P_δ (its moment of inertia about the origin).

Mean

$$\sum_{k=0}^{n-1} k P_{\delta}(k) \quad (12)$$

When $P_{\delta}(k)$ values are concentrated near the origin, mean is small and mean is large when they are far from the origin.

Entropy

$$-\sum_{k=0}^{(n-1)} k P_{\delta}(k) \quad (13)$$

Entropy is smallest when $P_{\delta}(k)$ values are unequal, and largest when $P_{\delta}(k)$ values are equal. Entropy is directly proportional to unpredictability.

The above-mentioned features were calculated for $\delta = (0, 1), (1, 1), (1, 0)$, and the total mean values on the four features were taken.

4.3 Run Length Matrix

Run length method allows extraction of higher order statistical texture features. Run length matrix, $P_{\theta}(i,j)$, records the frequency that j points with a gray level i continue in the direction θ . The $(i)^{th}$ dimension of the matrix corresponds to the gray level and has a length equal to the maximum gray level, n , while $(j)^{th}$ corresponds to the run length and has length equal to the maximum run length, l . Five measures from run-length matrixes of $\theta = 0^{\circ}, 45^{\circ}, 90^{\circ}$, and 135° were computed by as follows.

Short Run Emphasis



$$(14)$$

Short run lengths are emphasized by dividing each run length value by the square of its length. The total number of runs in the image is the denominator.

Long run emphasis



$$(15)$$

In order to allow higher weight to the long runs, each run length value is multiplied by the square of its length.

Run Percentage

$$\frac{\sum_i \sum_j P_{\theta}(i, j)}{A} \quad (16)$$

A is the area of the image. This particular feature is the ratio between the total number of observed runs in image and the total number of possible runs if all runs had a length of one.

Gray Level Non-uniformity



$$(17)$$

This feature depends on high run length values. The gray level non-uniformity feature

will have its lowest value if the runs are evenly distributed over all gray levels.

Run Length Non-uniformity:



$$(18)$$

This feature will be the lowest if the runs are evenly distributed over all runs length.

5. Classifier

5.1 Naïve Baye Classifier

Naïve Baye classification is a type of classification that enable categorizing of test samples with many variables and classes, without requiring a large number of observations for each possible combination of variables. Variables, or features are assumed to be independent from one another and the probability that the sample belongs to a specific feature is calculated individually.

Bayes Theorem

Let X be the data record (case) whose class label is unknown. Let H be some hypothesis, such as "data record X belongs to a specified class C." For classification, we want to determine P (H|X) -- the probability that the hypothesis H holds, given the observed data record X. P (H|X) is the posterior probability of H conditioned on X. For example, the probability that a fruit is an apple, given the condition that it is red and round. In contrast, P(H) is the prior probability, or apriori probability, of H. In this example P(H) is the probability that any given data record is an apple, regardless of how the data record looks. The posterior probability, P (H|X), is based on more information (such as background knowledge) than the prior probability, P(H), which is independent of Similarly, P (X|H) is posterior probability of X conditioned on H. That is, it is the probability that X is red and round given that we know that it is true that X is an apple. P(X) is the prior probability of X, i.e., it is the probability that a data record from our set of fruits is red and round. Bayes theorem is useful in that it provides a way of calculating the posterior probability, P(H|X), from P(H), P(X), and P(X|H). [28]. Bayes theorem is

$$P (H|X) = P(X|H) P(H) / P(X)$$

5.2 K-Nearest Neighbour Classifier

K-Nearest Neighbours (K-NN) algorithm is a non-parametric method where the proximity of neighbouring input (x) observations in the training data set and their corresponding output values (y) are used to predict the output values of cases in the testing data set.

Euclidean distance between 2 input vectors x_1 and x_2 are computed as length of the difference vector $x_1 - x_2$, denoted by the equation:

$$d(x_r, x_s) = |x_r - x_s| = \sqrt{(x_{r1} - x_{s1})^2 + (x_{r2} - x_{s2})^2}$$

For distance between two p-dimensional vectors $u = (u_1, u_2, \dots, u_p)$ and $v = (v_1, v_2, \dots, v_p)$ is calculated as:

$$d(u, v) = |u - v| = \sqrt{(u_1 - v_1)^2 + (u_2 - v_2)^2 + \dots + (u_p - v_p)^2}$$

K-NN algorithm calculates and Euclidean distance between the test data and the training data individually. The validation of the test data is classified according to the closest neighbour training data and labelled the class of the nearest training data. In figure 3, the test data X has the closest proximity to training data C compared to training data A and B. Therefore it is classified as a Class 2.

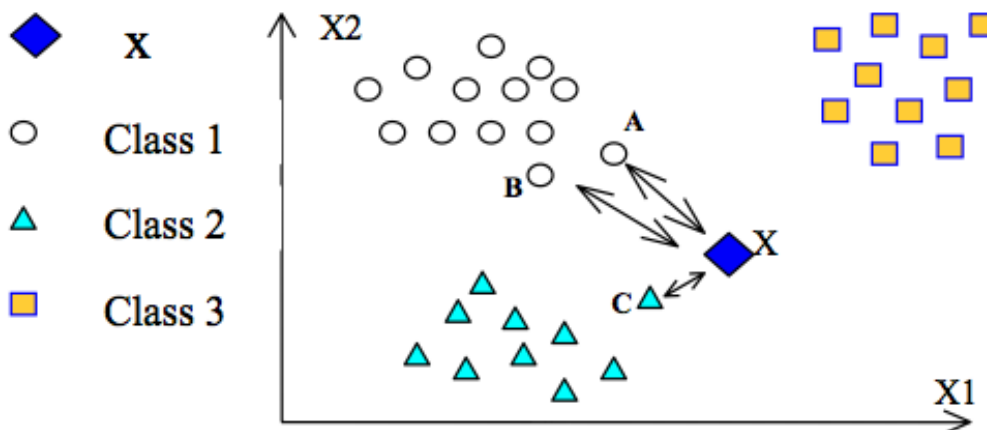


Figure 3: KNN Classification

Optimal K-NN model can be tuned to optimize accuracy of the model by tuning the parameter of K, neighbourhood size and optimal cut-off probability for each of the neighbour size. As K increases, k samples will start to resemble the probability density of each class in the local region of unknown measurement. Thus k-NNR is useful when there are many training samples available and k is set to a large value. If data samples are fairly spread out, there may be insufficient K samples in a small region, spreading out the region of interest in the attempt to contain K samples but sacrificing accuracy of estimation of probability. Therefore it is advisable to set K small.

6. Experimental Result:

A total of 108 image samples were used in this project, which were sorted out in their 3 class: Normal, NPDR and PDR.

Type	No of Samples
Normal	30
NPDR	49
PDR	31

Table 1: Class and number of image samples

pixel values of the region to 0. Once the image is prepared, it is again being process by median filtering to remove any unwanted impulse noise and lastly applying adaptive histogram to spread the histogram of the image across the range of values.

6.1 Classification

Using the data obtained from the images, their data are divided into two portions. Three different ratios are used during the training of classifiers

Training 1	30% Training/ 70% Testing
Training 2	70% Training/ 30% Testing
Training 3	30% Training (Random)/70% Testing

Table 2: Training Set and Ratio for testing and training.

The different classes for output and training are represented as numbers shown in the table below

Classes	Number
Normal	1
Non-PDR	2
PDR	3

Table 3: Class Labels

6.2 Results of Naïve Bayes Classifier

The table below is the breakdown of the number of images used for training and the accuracy of the Naïve Bayes Classifier

Training Set 1: 30% Training ; 70% Testing

Classes	No of data for training	No of data for testing	No of accurate data classification	Accuracy (%)
Normal	9	21	14	66.66
Non PDR	15	34	1	2.94
PDR	9	22	19	86.36
Total	33	77	43	44.16

Table 4: Results of Naïve Bayes Classifier (Training Set 1)

Training Set 2: 70% Training ; 30 % Testing

Classes	No of data for training	No of data for testing	No of accurate data classification	Accuracy (%)
Normal	21	9	9	100
Non PDR	34	15	4	26
PDR	22	9	7	77.77
Total	77	33	20	60.61

Table 5: Results of Naïve Bayes Classifier (Training Set 2)

Training Set 3: 30% Training (Random); 70% Testing

Classes	No of data for training	No of data for testing	No of accurate data classification	Accuracy (%)
Normal	9	21	1	4.76
Non PDR	15	34	33	97.06
PDR	9	22	4	18.18
Total	33	77	38	49.35

Table 6: Results of Naïve Bayes Classifier (Training Set 3)

The table as shown below is the breakdown of the images according to the actual class and the class predicted by Naive Bayes Classifier

Training Set 1

Predicted True	Normal	Non-PDR	PDR
Normal	14	7	0
Non-PDR	1	1	32
PDR	0	3	19

Table 7: Breakdown Results of Naïve Bayes Classifier (Training Set 1)

Training Set 2

Predicted True	Normal	Non-PDR	PDR
Normal	9	0	0
Non-PDR	2	4	9
PDR	0	2	7

Table 8: Breakdown Results of Naïve Bayes Classifier (Training Set 2)

Training Set 3

Predicted True	Normal	Non-PDR	PDR
Normal	1	20	0
Non-PDR	0	33	1
PDR	0	18	4

Table 9: Breakdown Results of Naïve Bayes Classifier (Training Set 3)

6.3 Results of K-Nearest Neighbour

The table below is the breakdown of the classes used for training and the accuracy of the K-NN Classifier

Training Set 1

Classes	No of data for training	No of data for testing	No of accurate data classification	Accuracy (%)
Normal	9	21	18	85.71
Non PDR	15	34	31	91.18
PDR	9	22	15	68.18
Total	33	77	64	83.11

Table 10: Results of KNN Classifier (Training Set 1)

Training Set 2

Classes	No of data for training	No of data for testing	No of accurate data classification	Accuracy (%)
Normal	21	9	9	100
Non PDR	34	15	14	93.33
PDR	22	9	8	88.88
Total	77	33	31	93.93

Table 11: Results of KNN Classifier (Training Set 2)

Training Set 3

Classes	No of data for training	No of data for testing	No of accurate data classification	Accuracy (%)
Normal	9	21	21	100
Non PDR	15	34	27	79.41
PDR	9	22	13	59.09
Total	33	77	61	72.72

Table 12: Results of KNN Classifier (Training Set 3)

The table as shown below is the breakdown of the images according to the actual class and the class predicted by K-NN Classifier

Training Set 1

Predicted	Normal	Non-PDR	PDR
True			
Normal	18	3	0
Non-PDR	0	31	3
PDR	0	7	15

Table 13: Breakdown Results of KNN Classifier (Training Set 1)

Training Set 2

Predicted	Normal	Non-PDR	PDR
True			
Normal	9	0	0
Non-PDR	0	14	1

PDR	0	1	8
-----	---	---	---

Table 14: Breakdown Results of KNN Classifier (Training Set 2)

Training Set 3

Predicted True	Normal	Non-PDR	PDR
Normal	21	0	0
Non-PDR	5	27	2
PDR	1	13	8

Table 15: Breakdown Results of KNN Classifier (Training Set 3)

7. Results and Discussion

Trials were conducted on the training of the classification, using non-normalised data in the classification. Results were much lower for both classifiers and the texture features selected that meets the probability criteria increase from 13 parameters to 14 parameters. The accuracy of the classifier drops approximately 10% overall for Naïve Bayes classifier, drop approximately 30% for K-Nearest Neighbour classifier. Normalization of all 3 classes of data was experimented, which provided similar results without normalization.

The result cant get accurate because of lack of data set or images availability. This accrucy can further be increased by introducing SVM classifier , Fuzzy control, ANN etc. It is suggested that a larger image database should be used as it will provide a much better accuracy as the expected accuracy of the classifier will be closer as the number of statistical data increases.

8. Reference List

1. Diabetic Statistic 2010, international diabetes federation. <http://www.scribd.com/doc/28061937/Diabetes-Statistics-2010>
2. National Health Survey 2004. Singapore: Epidemiology and Disease Control Division, Ministry of Health, 2004
3. WHO. Diabetes. <http://www.who.int/mediacentre/factsheets/fs312/en/index.html>
4. NUH, ophthalmology (Eye) Department: <http://www.nuh.com.sg/eye/patients-and-visitors/diseases-and-conditions/vitreo-retinal-diseases/diabetic-retinopathy.html>
5. St luke cataract and laser institute, Diabetic Retinopathy, condition <http://www.stlukeseye.com/Conditions/DiabeticRetinopathy.html>
6. The Retina of the human eye. <http://hyperphysics.phy-astr.gsu.edu/hbase/vision/retina.html>
7. WHO diabetics. <http://www.who.int/mediacentre/factsheets/fs312/en/index.html>
8. Department of optometry and vision science, University of melbourne eyecare, clinic facility. <http://www.university-eyecare.org.au/about/facilities.html>
9. Automatic Diagnosis Of Diabetic Retinopathy Using Fundus Images, Iqbal, M.I (771207-8638) Aibinu, A.M (730109-P554)Gubbal, N.S (820727-P639) Khan, A (801029-P212)
10. Xiaohui, Z., and Chutatape, O., ‘ Detection and classification of bright lesions in colour fundus Images’, Int. Conference on Image Processing, Vol 1, pp139-142, Oct 2004
11. Vallabha,D., Dorairaj, R., Namuduri K. R., and Thompson, H., "Automated Detection and

-
- Classification of Vascular Abnormalities in Diabetic Retinopathy", 38th Asilomar Conference on Signals, Systems and Computers, November 2004.
13. Background. <http://www.ocular-angiogenesis.nl/Background/Background.html>
 14. Automatic diagnosis of retinal diseases, D.Jayanthi, N.Devi, S.SwarnaParvathi, International Journal of Computer Science and Information Security,, Vol. 7, No. 1, 2010from color retinal images. <http://arxiv.org/ftp/arxiv/papers/1002/1002.2408.pdf>
 15. Digital image processing. Minakshi Kumar Photogrammetry and Remote Sensing Division Indian Institute of Remote Sensing, Dehra Dun <http://www.wamis.org/agm/pubs/agm8/Paper-5.pdf>
 16. Color Image Classification and Retrieval using Image mining Techniques Dr.V.Mohan, A.Kannan International Journal of Engineering Science and Technology Vol. 2(5), 2010, 1014-1020 <http://www.ijest.info/docs/IJEST10-02-05-50.pdf>
 17. Artificial neural network. http://viswiki.com/en/Artificial_neural_network
 18. Wikipedia. Support Vector Machine http://en.wikipedia.org/wiki/Support_vector_machine
 19. Digital Imaging Tutorial, Cornell University <http://www.library.cornell.edu/preservation/tutorial/intro/intro-01.html>
 20. R.C. Gonzalez, Richard E. Woods, "Digital Image Processing" Prentice Hall, 2002.
 21. Low vs High Resolution <http://www.gadgetell.com/tech/comment/apple-officially-announces-iphone-4.html>
 22. Wikipedia, Image Resolution http://en.wikipedia.org/wiki/Image_resolution
 23. Webstyle Guide, Colour Display <http://webstyleguide.com/wsg2/graphics/displays.html>
 24. P.F. Lammertsma "Histogram Equalization" 2006
 25. Lecture Notes," EE4266: Computer Vision " Nanyang Technological University
 26. Median Filter <http://tracer.lcc.uma.es/problems/mfp/mfp.html>
 27. The Handbook of Pattern Recognition and Computer Vision (2nd Edition), by C. H. Chen, L. F. Pau, P. S. P. Wang (eds.), pp. 207-248, World Scientific Publishing Co., 1998.
 28. A. Materka and M. Strzelecki, Texture analysis methods - a review, Tech. report, Institute of Electronics, Technical University of Lodz, 1998
 29. Papoulis, A. "Bayes' Theorem in Statistics" and "Bayes' Theorem in Statistics (Reexamined)." §3-5 and 4-4 in Probability, Random Variables, and Stochastic Processes, 2nd ed. New York: McGraw-Hill, pp. 38-39, 78-81, and 112-114, 1984.